THE JOURNAL OF BIOLOGICAL CHEMISTRY VOL. 284, NO. 38, pp. 25687–25696, September 18, 2009

New Insights into the Early Steps of Phosphatidylinositol Mannoside Biosynthesis in Mycobacteria

PimB′ IS AN ESSENTIAL ENZYME OF MYCOBACTERIUM SMEGMATIS[*][S]

Received for publication, June 5, 2009, and in revised form, July 24, 2009 Published, JBC Papers in Press, July 28, 2009, DOI 10.1074/jbc.M109.030593

Marcelo E. Guerin[1], **Devinder Kaur, B. S. Somashekar, Sara Gibbs, Petra Gest, Delphi Chatterjee, Patrick J. Brennan, and Mary Jackson**[2]

From the Department of Microbiology, Immunology, and Pathology, Colorado State University, Fort Collins, Colorado 80523-1682

Phosphatidyl-*myo*-inositol mannosides (PIMs) are key glycolipids of the mycobacterial cell envelope. They are considered not only essential structural components of the cell but also important molecules implicated in host-pathogen interactions. Although their chemical structures are well established, knowledge of the enzymes and sequential events leading to their biosynthesis is still incomplete. Here we show for the first time that although both mannosyltransferases PimA and PimB′ (MSMEG_4253) recognize phosphatidyl-*myo*-inositol (PI) as a lipid acceptor, PimA specifically catalyzes the transfer of a Man*p* residue to the 2-position of the *myo*-inositol ring of PI, whereas PimB′ exclusively transfers to the 6-position. Moreover, whereas PimB′ can catalyze the transfer of a Man*p* residue onto the PI-monomannoside (PIM_1) product of PimA, PimA is unable *in vitro* to transfer Man*p* onto the PIM_1 product of PimB′. Further assays using membranes from *Mycobacterium smegmatis* and purified PimA and PimB′ indicated that the acylation of the Man*p* residue transferred by PimA preferentially occurs after the second Man*p* residue has been added by PimB′. Importantly, genetic evidence is provided that *pimB′* is an essential gene of *M. smegmatis*. Altogether, our results support a model wherein Ac_1PIM_2, a major form of PIMs produced by mycobacteria, arises from the consecutive action of PimA, followed by PimB′, and finally the acyltransferase MSMEG_2934. The essentiality of these three enzymes emphasizes the interest of novel anti-tuberculosis drugs targeting the initial steps of PIM biosynthesis.

PIMs[3] are unique mannolipids found in abundant quantities in the inner and outer membranes of the cell envelope of *Mycobacterium* spp. and a few other actinomycetes.[4] They are based on a phosphatidyl-*myo*-inositol (PI) lipid anchor carrying one to six Man*p* residues and up to four acyl chains (for review see Refs. 1, 2). Based on a conserved mannosyl-PI anchor, they are also thought to be the precursors of the two major mycobacterial lipoglycans, lipomannan (LM) and lipoarabinomannan (LAM) (1, 2). PIMs, LM, and LAM are considered not only essential structural components of the mycobacterial cell envelope (3–6), but also important molecules implicated in host-pathogen interactions in the course of tuberculosis and leprosy (1).

Although the chemical structure of PIMs is now well established, knowledge of the enzymes and sequential events leading to their biosynthesis is still fragmentary. According to the currently accepted model, the biosynthetic pathway is initiated by the transfer of two Man*p* residues and a fatty acyl chain to PI in the cytoplasmic leaflet of the plasma membrane. Based on genetic and biochemical evidence, Korduláková *et al.* (5) identified PimA (MSMEG_2935 in *Mycobacterium smegmatis* mc^2155) as the enzyme that catalyzes the first mannosylation step of the pathway transferring a Man*p* residue most likely to the 2-position of the *myo*-inositol (*myo*-Ins) ring of PI. In contrast, the identity of PimB′, the enzyme responsible for the transfer of the second Man*p* to the 6-position of the *myo*-Ins ring of PIM_1, still remains controversial. The Rv0557 protein of *Mycobacterium tuberculosis* H37Rv (PimB; MSMEG_1113 in *M. smegmatis* mc^2155) was originally characterized as PimB′ (7). However, the lack of an *Rv0557* ortholog in the genome of *Mycobacterium leprae* and the fact that the disruption of this gene in *M. tuberculosis* Erdman did not significantly affect the biosynthesis of PIMs suggest that compensatory activities exist in the bacterium or that *Rv0557* serves another primary function (8, 9). Somewhat supporting the latter hypothesis, the ortholog of *Rv0557* in *Corynebacterium glutamicum* (*NCgl0452*, renamed *mgtA*) was implicated in the mannosylation of a novel glycolipid (1,2-di-*O*-C_{16}/$C_{18:1}$-(α-D-mannosyl)-(1→4)-(α-D-glucopyranosyluronic acid)-(1→3)-glycerol), and Rv0557 from *M. tuberculosis* was reported to functionally complement for this enzyme in a *C. glutamicum* knock-out mutant (10). However, to our knowledge this mannosylated glycolipid has never been reported in mycobacteria, and it remains unclear whether PimB serves a similar physiological function in *Mycobacterium* spp.

* This work was supported, in whole or in part, by National Institutes of Health Grant AI064798 from NIAID.

[S] The on-line version of this article (available at http://www.jbc.org) contains supplemental text and Figs. 1S–8S.

[1] To whom correspondence may be addressed. Tel.: 970-491-4067; Fax: 970-491-1815; E-mail: mrcguerin@gmail.com.

[2] To whom correspondence may be addressed. Tel.: 970-491-4067; Fax: 970-491-1815; E-mail: Mary.Jackson@colostate.edu.

[3] The abbreviations used are: PIM, phosphatidyl-*myo*-inositol mannoside; Man*p*, mannopyranosyl; ManT, mannosyltransferase; MALDI-TOF, matrix-assisted laser desorption-ionization time-of-flight; PI, phosphatidyl-*myo*-inositol; LM, lipomannan; LAM, lipoarabinomannan; *myo*-Ins, *myo*-inositol.

[4] PIM is used to describe the global family of phosphatidylinositol mannosides that carries one to four fatty acids (attached to the glycerol, inositol, and/or mannose) and one to six mannose residues. In Ac_xPIM_y, *x* refers to the number of acyl groups esterified to available hydroxyls on the mannose or *myo*-inositol residues, and y refers to the number of mannose residues.

More recently, Lea-Smith *et al.* (11) have shown that the biosynthesis of Ac_1PIM_2 from Ac_1PIM_1 in *C. glutamicum* is catalyzed by NCgl2106 (Cg-PimB′). Disruption of the *NCgl2106* gene totally abolished Ac_1PIM_2 production in the mutant, arguing against the existence of a compensatory activity associated with the corynebacterial PimB enzyme. Although Ac_1PIM_2 production in *Cg-pimB′* and *Cg-pimB′*/*Cg-pimB* knock-out mutants was restored upon complementation with the *M. tuberculosis Rv2188c* gene (11, 12), direct evidence that *Rv2188c* carried out the same physiological function in mycobacteria has been lacking. Moreover, in light of the recent work by Torrelles *et al.* (9) showing an involvement of *pimB* (*Rv0557*) in the synthesis of LM and LAM in *M. tuberculosis* Erdman and of the demonstrated relaxed substrate specificity of the *M. tuberculosis* PimB (Rv0557) and PimB′ (Rv2188c) enzymes expressed in *C. glutamicum* (12), whether or not *pimB* and *pimB′* could compensate for one another in mycobacteria remained open to speculation.

Both PIM_1 and PIM_2 can be acylated with palmitate at position 6 of the Man*p* residue transferred by PimA by the acyltransferase MSMEG_2934 (orthologous to Rv2611c from *M. tb*) to form Ac_1PIM_1 and Ac_1PIM_2, respectively (13). Ac_1PIM_2 can further be acylated at position 3 of the *myo*-Ins ring by an as yet unidentified acyltransferase to yield Ac_2PIM_2. Importantly, Ac_1PIM_2 and Ac_2PIM_2 are among the most abundant forms of PIMs found in mycobacteria and are considered both metabolic end products and intermediates in the biosynthesis of more polar forms of PIMs (PIM_5 and PIM_6), LM, and LAM.

In this work, clear evidence is provided that PimB′ (MSMEG_4253 in *M. smegmatis* mc^2155) is the α-ManT responsible for the biosynthesis of PIM_2 from PIM_1 in mycobacteria and that no other ManT can compensate for a deficiency in this enzyme in *M. smegmatis*. Like PimA (5), PimB′ is essential to the growth of *M. smegmatis*. Cell-free assays using purified PimA and PimB′ and *M. smegmatis* membrane preparations provide new insights into the sequential events leading to the synthesis of the early forms of PIMs in mycobacteria.

EXPERIMENTAL PROCEDURES

Cloning, Expression, and Purification of PimB′ from M. smegmatis in Escherichia coli—The *M. smegmatis pimB′* gene (*MspimB′*, *MSMEG_4253*, 72% amino acid identity to Rv2188c) was amplified from genomic *M. smegmatis* mc^2155 DNA by standard PCR using oligonucleotide primers pimB′_NdeI_Fwd (5′-GGAATTCCATATGACCCGGGTGTTGTTGGTCACC-3′, pimB′_XhoI_Rev (5′-CCGCTCGAGCGCCTGACGCGCCTCGCGTCGG-3′), and Phusion DNA Polymerase (New England Biolabs). The PCR fragment was digested with NdeI and XhoI and ligated to the corresponding restriction sites of pET29a (Novagen) generating pET29a-*MspimB′*. The recombinant *Ms*PimB′ protein (385 residues) has an additional peptide of eight amino acids (^{386}LEHHHHHH^{393}) at the C terminus that includes a histidine tag.

E. coli BL21(DE3)pLysS cells transformed with pET29a-*MspimB′* were grown in 2× YT medium supplemented with 25 μg ml^{-1} kanamycin and 34 μg ml^{-1} chloramphenicol at 37 °C. *MspimB′* expression was induced by adding 0.5 mM isopropyl 1-thio-β-D-galactopyranoside (MP Biomedicals). After 4 h at 37 °C, cells were harvested and resuspended in solution A (50 mM Tris-HCl, pH 8.0) containing protease inhibitors (Complete EDTA-free, Roche Applied Science). Cells were disrupted by sonication (five cycles of 1 min), and the suspension was centrifuged for 20 min at 10,000 × *g*. The supernatant was applied to a HisTrap chelating column (1 ml; GE Healthcare) equilibrated with solution B (50 mM Tris-HCl, pH 8.0, 500 mM NaCl). The column was then washed with solution B until no absorbance at 280 nm was detected. Elution was performed with a linear gradient of 0–500 mM imidazole in solution B at 1 ml min^{-1}. The resulting preparation displayed a single protein band when run on a 10% SDS-polyacrylamide gel stained with Coomassie Brilliant Blue (supplemental Fig. 1S). The purified enzyme was concentrated to 10 mg ml^{-1} in solution A containing 20% glycerol and stored at −80 °C until further use in enzyme assays.

Enzyme Assays—The enzymatic activity of *Ms*PimA and *Ms*PimB′ was monitored using a radiometric assay. The reaction mixture contained 0.0625 μCi of GDP-[C^{14}]Man (specific activity, 305 mCi mmol^{-1}; Amersham Biosciences), 10 μg of PI (Avanti Polar Lipids; liver PI, $[M - H]^-$, m/z = 885.53, where the predominant species contains one polyunsaturated C_{20} and one C_{18} fatty acyl chain), 50 μg of purified *Ms*PimA, *Ms*PimB′, or a mix of *Ms*PimA and *Ms*PimB′ and 50 mM Tris-HCl, pH 7.5, in a final volume of 250 μl. In some assays, membrane preparations from *M. smegmatis* mc^2155 (0.5 mg of proteins) served as the source of lipid acceptors. Reactions were incubated for 2 h at 37 °C and stopped with 1.5 ml of $CHCl_3/CH_3OH$ (2:1, by volume). The PIM-containing organic phase was prepared and analyzed by TLC as described by Korduláková *et al.* (5). *Ms*PimA was purified as described previously (14).

For structural analyses, 500 μM cold GDP-Man replaced GDP-[C^{14}]Man in the assay mixture described above. The reactions were incubated overnight at 37 °C and stopped by adding 1.5 ml of $CHCl_3/CH_3OH$ (2:1, by volume). The nonradioactive mannolipid products from 15 reactions were isolated by preparative TLC as described (5).

Matrix-assisted Laser Desorption Ionization Time-of-Flight Mass Spectrometry—Compounds 1–5 were mixed with an equal volume of matrix (2,5-dihydroxylbenzoic acid dissolved in 10 mg ml^{-1} acetonitrile/water, 50:50, 0.1% trifluoroacetic acid), and the molecular mass was measured in the negative ion mode by MALDI-TOF MS on a Bruker Ultraflex TOF/TOF mass spectrometer (Bruker Daltonics, Billerica, MA). External calibration was performed using an eight component calibration mixture on a spot adjacent to the sample.

NMR Analysis—One-dimensional and two-dimensional NMR experiments were carried out at 25 °C in a Varian Inova 500-MHz NMR spectrometer (Varian Inc., Palo Alto, CA) using an HCN probe head equipped with shielded z-gradient. Samples were dissolved in 0.6 ml of $CHCl_3/CD_3OD$ (2:1, by volume) and spectra acquired using a 5-mm NMR probe. Typical parameters used for one-dimensional ^{1}H experiments were as follows: sweep width, 5500Hz; flip angle, 45°; time domain data points, 32,768; number of transients, 32 or 256; and relaxation delay, 1.5 s. For the complete structural analysis of PIM_1, PIM_2, and Ac_1PIM_2, two-dimensional experiments, including gradient-selected correlation spectroscopy, total correlation

spectroscopy, heteronuclear single quantum coherence spectroscopy, and heteronuclear multiple bond correlation spectroscopy were carried out. Parameters used for two-dimensional correlation spectroscopy and total correlation spectroscopy were as follows: sweep width, 5500 Hz in both *F*2 and *F*1 dimensions; time domain data points, 2048; number of free induction decay with t_1 increment, 512; number of transients, 32 or 256; and relaxation delay, 1.5s. Parameters used for heteronuclear single quantum coherence and heteronuclear single quantum coherence spectroscopy were as follows: sweep width, 5500 Hz in *F*2 and 30,188 Hz in *F*1; time domain data points, 2048; number of free induction decays with t_1 increment, 256; number of transients, 32 or 256; and relaxation delay, 1.5 s. The acquired NMR data were processed using the TOPSPIN 2.1 software (Bruker GmbH, Karlsruhe, Germany).

Construction of M. smegmatis MspimB′ Conditional Mutant—Essentially the same strategy was used to construct a conditional *MspimB′* mutant of *M. smegmatis* as was used earlier to generate an *MspimA* conditional mutant (5). The *M. smegmatis MspimB′* gene (*MSMEG_4253*) and flanking regions were amplified from genomic *M. smegmatis* mc^2155 DNA by standard PCR strategies using oligonucleotide primers *Ms*pimB′_KO_ApaI_fwd (5′-ATAATGGGCCCGCAAAACTGCGTGACCTGTACG-3′) and *Ms*pimB′_KO_SpeI_rev (5′-ATTATACTAGTGACCTCGGCGCCATCGACG-3′), and Phusion DNA polymerase (New England Biolabs). A disrupted allele of *MspimB′*, *MspimB′*::*km*, was constructed by cloning the kanamycin resistance cassette from pUC4K (GE Healthcare) into the AgeI and StuI sites of *MspimB′*, generating a 363-bp deletion within the coding sequence of *MspimB′*. *MspimB′*::*km* was then ligated to pJQ200*xylE* to yield pJQ*MspimB′KX*, the vector used to achieve allelic replacement at the *MspimB′* locus (5). The temperature-sensitive pCG76 derivative (15), pCG*MspimB′*, was used as the rescue plasmid to carry a functional copy of the *MspimB′* gene in the conditional mutant.

Homology Modeling of MsPimB′—Homology modeling of *Ms*PimB′ was performed with MODELLER 9 Version 4 (16) using the atomic coordinates of *Ms*PimA complexed with GDP-Man (Protein Data Bank code 2GEJ (17)) as a template. Sequence alignment was carried out manually to match functionally conserved residues, predicted secondary structures, and hydrophobicity profiles. Secondary structures were predicted using the Jpred program (18). The models were assessed by the VERIFY_3D program.

RESULTS AND DISCUSSION

MsPimB′ Catalyzes in Vitro the Transfer of a Manp Residue to the 6-Position of the Myo-Ins Ring of PI—With the goal of determining the function of the mycobacterial PimB′ enzyme, a recombinant form of the *M. smegmatis* protein (*Ms*PimB′) with a C-terminal histidine tag was produced in *E. coli* BL21(DE3)pLysS and purified to near homogeneity (supplemental Fig. 1S). As had been the case with the *M. tuberculosis* PimA protein earlier (5, 14, 17), attempts to produce the PimB′ enzyme from *M. tuberculosis* yielded relatively small amounts of soluble protein compared with the *M. smegmatis* version, and these efforts were thus not pursued further.

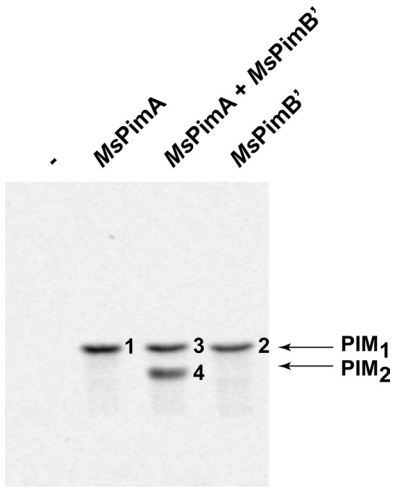

FIGURE 1. ***In vitro* synthesis of PIM_1 and PIM_2 by purified recombinant forms of *Ms*PimA and *Ms*PimB′.** TLC autoradiograph of reactions performed with purified recombinant *Ms*PimA, *Ms*PimB′, or a mix of *Ms*PimA and *Ms*PimB′ (1:1 by weight) using GDP-[C^{14}]Man and commercial PI as the donor and acceptor substrates, respectively.

ManT assays were then run using different combinations of the purified *Ms*PimA and *Ms*PimB′ enzymes. When commercial liver PI and GDP-[^{14}C]Man served as the acceptor and donor substrates in the assay, purified *Ms*PimA (14) catalyzed the formation of PIM_1 (*mannolipid 1,* Fig. 1). Unexpectedly, the formation of a ^{14}C-labeled mannolipid with an R_f similar to that of PIM_1 was also observed when purified *Ms*PimB′ was used as the source of enzyme in the assay (*mannolipid 2*, Fig. 1). To further characterize mannolipids 1 and 2, nonradioactive products were purified by preparative TLC from reaction mixtures in which cold GDP-Man replaced GDP-[C^{14}]Man. MALDI-TOF-MS analyses in the negative ion mode confirmed compounds 1 ($[M - H]^-$, m/z = 1047.60) and 2 ($[M - H]^-$, m/z = 1047.65) as PIM_1 molecules (the $[M - H]^-$ m/z value of the commercial liver PI is 885.53) (supplemental Fig. 2S). *Ms*PimB′ thus has the ability *in vitro* to transfer Man*p* from GDP-Man onto PI, generating PIM_1.

A combination of one-dimensional and two-dimensional NMR was then used to determine the position at which the Man*p* residues were attached to *myo*-Ins in mannolipids 1 and 2 (for details see supplemental material and supplemental Figs. 3S–6S) (19–21). As depicted in Fig. 2, the ^{1}H NMR spectra of mannolipid 1 shows one peak at 5.14 ppm assigned to the α-anomeric proton of the Man*p* residue attached to position 2 of *myo*-Ins. The ^{1}H and ^{13}C chemical shift values of mannolipid 3 is exactly comparable with that of mannolipid 1, and therefore compound 3 was also assigned to 2-linked PIM_1. In the spectra of compound 2, the peak at 5.072 ppm was assigned as the α-anomeric proton of the Man*p* residue attached to position 6 of *myo*-Ins. The ^{1}H NMR spectra of mannolipid 4 shows two distinct peaks at 5.129 and 5.046 ppm assigned to α-anomeric protons of two Man*p* residues attached to the 2- and 6-positions of *myo*-Ins.

For the first time, direct evidence arising from the use of purified enzymes was thus provided that *Ms*PimA catalyzes the transfer of a Man*p* residue from GDP-Man*p* to the 2-position of the *myo*-Ins ring of PI, and *Ms*PimB′ catalyzes the transfer of a Man*p* residue to the 6-position.

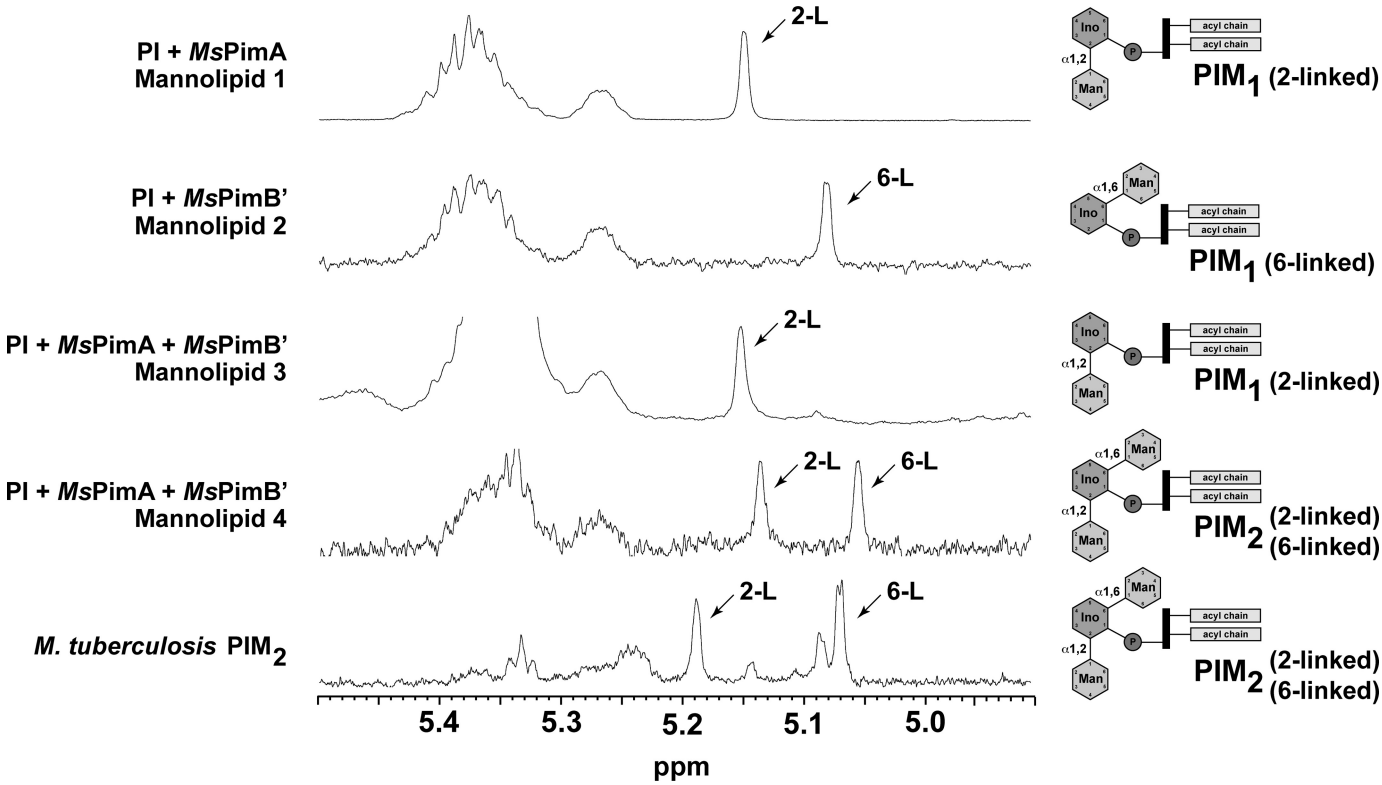

FIGURE 2. **NMR analysis of purified mannolipids.** ^{1}H NMR spectra of mannolipids 1–4. The ^{1}H NMR spectra of mannolipid 1 shows one peak at 5.14 ppm assigned to the α-anomeric proton of the Man*p* residue attached to position 2 of *myo*-Ins. The ^{1}H and ^{13}C chemical shift values of mannolipid 3 are exactly comparable with that of mannolipid 1, and therefore compound 3 was also assigned to 2-linked PIM_1. In the spectra of compound 2, the peak at 5.072 ppm was assigned as the α-anomeric proton of the Man*p* residue attached to position 6 of *myo*-Ins. The ^{1}H NMR spectra of mannolipid 4 shows two distinct peaks at 5.129 and 5.046 ppm assigned to α-anomeric protons of two Man*p* residues attached to distinct positions of *myo*-Ins. Based on the combined two-dimensional NMR spectral analyses, the α-anomeric protons at 5.129 and 5.046 ppm are assigned to the peaks that are 2- and 6-linked to *myo*-Ins, respectively, and therefore, compound 4 is assigned to 2,6-linked PIM_2 (see supplemental material and supplemental Figs. 3S–6S).

Sequential Order of the Mannosylation Reactions Leading to the Formation of PIM_2 from PI and GDP-Man—The simultaneous addition of purified *Ms*PimA and *Ms*PimB′ (1:1, w/w) to the reaction mixture described above yielded two products, mannolipid 3 and mannolipid 4 (Fig. 1). MALDI-TOF-MS analyses in the negative ion mode confirmed compound 3 ($[M - H]^-$, $m/z = 1047.60$) as PIM_1 and compound 4 as PIM_2 ($[M - H]^-$, $m/z = 1209.71$) (supplemental Fig. 2S). From this experiment, it can thus be concluded that *Ms*PimA and *Ms*PimB′ are sufficient for the formation of PIM_2 from PI and GDP-Man to occur. The fact that no PIM_3 or more mannosylated products were formed in the reaction even after prolonged incubation times further indicated that *Ms*PimA and *Ms*PimB′ are unable to mannosylate PIM products beyond PIM_2. Thus *Ms*PimA and *Ms*PimB′ appear to each catalyze the transfer of one single Man*p* residue.

To determine the sequence of the reactions leading to the formation of PIM_2, two independent assays were carried out in which purified *Ms*PimA and *Ms*PimB′ were added sequentially to the reaction mixture. In one of the assays, *Ms*PimA was added first to a reaction mixture containing PI and GDP-[C^{14}]Man. After 2 h of incubation, one-half of the reaction was stopped by the addition of $CHCl_3/CH_3OH$ (2:1), and the other half was incubated at 60 °C for 15 min to inactivate the enzyme. Purified *Ms*PimB′ was then added to the heat-inactivated assay mixture, and the reaction allowed to proceed overnight at 37 °C. In the second assay, *Ms*PimB′ was added first to the reaction mixture, then inactivated as described above, and *Ms*PimA finally added. That both *Ms*PimA and *Ms*PimB′ were inactivated by heat treatment was verified by running independent assays with each of the purified enzymes (supplemental Fig. 7S). Consistent with our previous results, both *Ms*PimA and *Ms*PimB′ catalyzed the transfer of a Man*p* residue from GDP-Man to PI to form PIM_1 (Fig. 3*A*). The subsequent addition of *Ms*PimB′ to the *Ms*PimA reaction mixture clearly led to the synthesis of ^{14}C-labeled PIM_2 (Fig. 3*A*). In striking contrast, the addition of *Ms*PimA to the *Ms*PimB′ reaction mixture only resulted in the stimulation of PIM_1 production with no detectable formation of PIM_2 (Fig. 3*A*). We thus conclude from this experiment that although *Ms*PimB′ recognizes the PIM_1 product of *Ms*PimA (with an α-1,2-linked Man*p* residue on the *myo*-Ins ring; Fig. 2) as an acceptor substrate, *Ms*PimA is unable to transfer a Man*p* residue onto a PIM_1 product bearing an α-1,6-linked Man*p* residue.

With the transfer of Man*p* from GDP-Man onto PI catalyzed by *Ms*PimB′ occurring 53 times slower than both the *Ms*PimA-dependent transfer of Man*p* onto PI and the *Ms*PimB′-dependent addition of Man*p* onto PIM_1 (Fig. 3, *B* and *C*), it is clear that the different activities of the two enzymes with PI and, subsequently, PIM_1 acceptors dictate the order in which the mannosylation of PI and PIM is to occur under physiological conditions. In further support of this assumption, the PIM_1 product

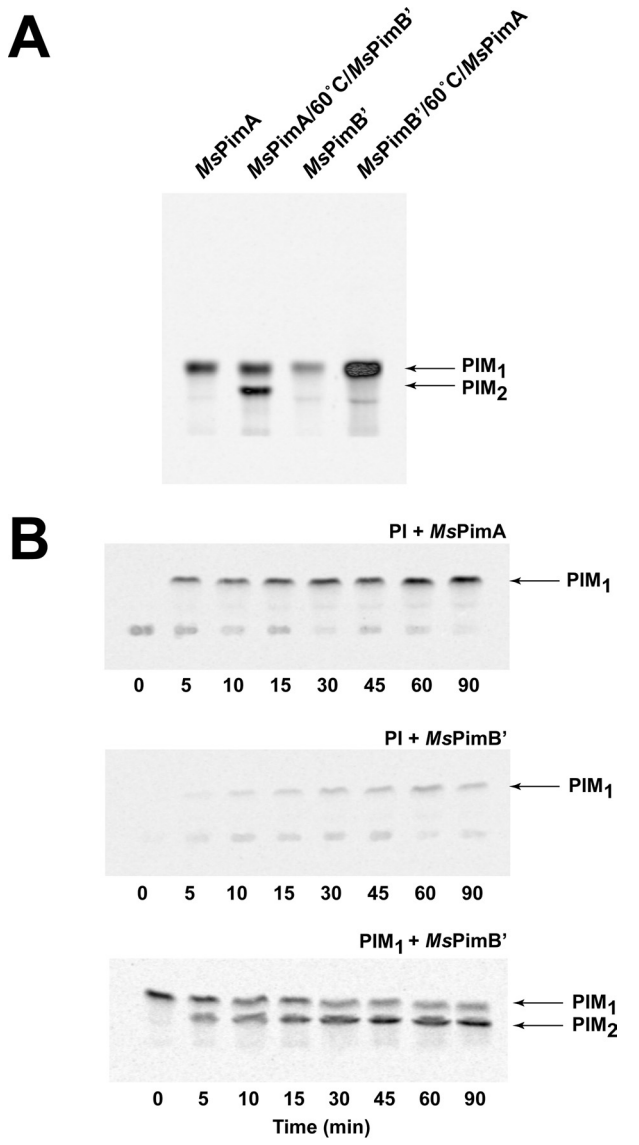

FIGURE 3. **PIM_2 is produced by the sequential addition of mannosyl residues to PI and PIM_1 transferred by *Ms*PimA and *Ms*PimB′, respectively.** *A,* TLC autoradiograph of enzymatic reactions performed with purified recombinant *Ms*PimA and *Ms*PimB′ added sequentially to the reaction mixture. GDP-[C^{14}]Man and commercial PI served as the donor and acceptor substrates in these reactions (see text for details). *B,* time course of transfer of [C^{14}]Man*p* from GDP-[C^{14}]Man onto PI and PIM_1 (carrying an α-1,2-linked Man*p* residue) by *Ms*PimA and *Ms*PimB′. *C,* quantification of the reaction products shown in *B*. *Solid circles*, PIM_1 product of *Ms*PimA; *solid squares*, PIM_2 product of *Ms*PimB′; *open circles*, PIM_1 product of *Ms*PimB′.

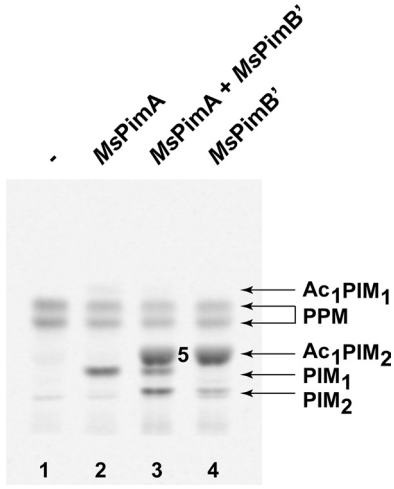

FIGURE 4. **Effects of adding purified *Ms*PimA, *Ms*PimB′, or both enzymes on the synthesis of PIMs by membrane preparations from *M. smegmatis*.** Assays were carried out as described in the text using GDP-[C^{14}]Man as the donor substrate and *M. smegmatis* membranes as a natural source of phospho(glyco)lipid acceptors. TLC autoradiograph of the reactions: *lane 1,* no purified enzyme was added; *lane 2,* purified *Ms*PimA was added; *lane 3,* equal amounts of purified *Ms*PimA and *Ms*PimB′ were added simultaneously; *lane 4,* purified *Ms*PimB′ was added.

(*mannolipid 3,* Fig. 1) formed in a competition assay, where equal amounts of *Ms*PimA and *Ms*PimB′ were used as enzyme sources, exclusively consisted of α-1,2-linked Man*p* residues, as opposed to the expected mixture of α-1,2- and α-1,6-linked Man*p* residues if both enzymes had transferred Man*p* onto PI with comparable efficiencies (Fig. 2).

MsPimB′ Stimulates the Production of Ac_1PIM_2 in M. Smegmatis Membrane Preparations—When membranes prepared from *M. smegmatis* mc^2155 were used as a source of phospho(glyco)lipid acceptor, the addition of purified *Ms*PimA clearly stimulated the synthesis of PIM_1, accompanied by the accumulation of small amounts of Ac_1PIM_1 (Fig. 4, *lane 2*). The addition of *Ms*PimB′ to the membrane preparations, in contrast, led to an even greater accumulation of a compound (*mannolipid 5*) with R_f properties similar to that of Ac_1PIM_2 (Fig. 4, *lane 4*). MALDI-TOF MS and NMR analyses confirmed the identity of this product as Ac_1PIM_2 containing two C_{16} and one C_{19} fatty acyl chains ($[M - H]^-$, $m/z = 1413.88$) (supplemental Fig. 2S) (21), among which two fatty acyl chains are carried by the glycerol moiety and one acyl chain is attached to Man*p* residue located at position 2 of the *myo*-Ins ring (supplemental Fig. 8S). The acylation of the Man*p* residue transferred by PimA is thought to result from the action of the acyltransferase encoded by *MSMEG_2934* in *M. smegmatis* mc^2155 (13).

Overall, the abundant *de novo* synthesis of Ac_1PIM_2 in the assay mixture containing purified *Ms*PimB′ (Fig. 4, *lane 4*) suggests that significant amounts of PIM_1 are available in the membranes of *M. smegmatis* or that the synthesis of this acceptor substrate is stimulated by the addition of purified *Ms*PimB′ to the reaction mixture. This observation and the fact that radiolabeled Ac_1PIM_2 was on the contrary not detectable in the assay mixture in which only purified *Ms*PimA was added (Fig. 4, *lane 2*) suggest that the physiological amounts of *Ms*PimB′ present in the membranes of *M. smegmatis* may be rate-limiting in the formation of PIM_2/Ac_1PIM_2. On the other hand, with almost

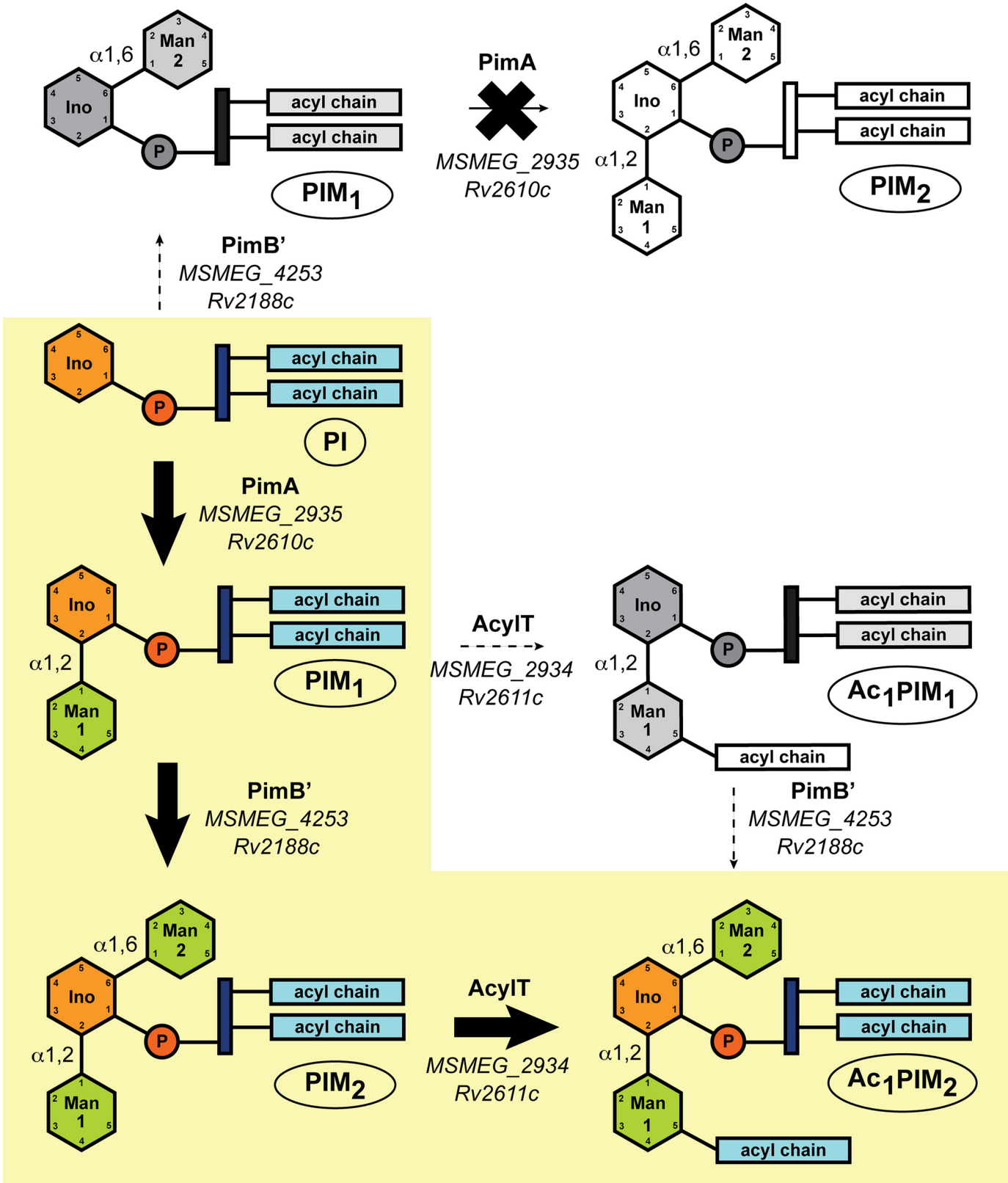

FIGURE 5. **Proposed pathway for the early steps of PIM biosynthesis in mycobacteria.** The two pathways originally proposed for the biosynthesis of Ac_1PIM_2 in mycobacteria are shown. (i) PI is mannosylated to form PIM_1. PIM_1 is then mannosylated to PIM_2, which is acylated to form Ac_1PIM_2. (ii) PIM_1 is first acylated to Ac_1PIM_1 and then mannosylated to Ac_1PIM_2. Our experimental evidence indicates that although both pathways might co-exist in mycobacteria (13), the sequence of events PI → PIM_1 → PIM_2 → Ac_1PIM_2 is favored. As an important part of the literature concerning PIM studies refers to the nomenclature based on the *M. tuberculosis* H37Rv sequences, the Rv numbers of the proteins are also included.

all of the PIM_2 product of *Ms*PimB′ being instantly converted to Ac_1PIM_2 (Fig. 4, *lane 4*), the activity of the acyltransferase does not seem to be limiting in the membranes of *M. smegmatis*. In fact, saturation of this enzyme only became clearly visible when both purified *Ms*PimA and *Ms*PimB′ were added to the reaction mixture, resulting in the accumulation of abundant quantities of PIM_1 and PIM_2 (Fig. 4, *lane 3*). Finally, the quasi-exclusive occurrence of PIM_2s under their acylated form (Ac_1PIM_2) in the assay where *Ms*PimB′ was added (Fig. 4, *lane 4*), whereas the product of the reaction catalyzed by *Ms*PimA essentially occurred as PIM_1 (*i.e.* with no acylation on the Man*p* residue) (Fig. 4, *lane 2*), strongly suggests that the acyltransferase MSMEG_2934 preferentially acylates PIM_2 over PIM_1. Thus, despite MSMEG_2934 displaying acyltransferase activity on both PIM_1 and PIM_2 *in vitro* (13), it is likely that under physiological conditions the preferred pathway to Ac_1PIM_2 involves the transfer of both mannosyl residues onto PI prior to the acylation of the α-1,2-linked Man*p* residue.

Revised Model for the Early Steps of PIM Biosynthesis—Based on present experimental evidence, a revised model for the early steps of PIM biosynthesis is presented in Fig. 5. As inferred from previous studies (5, 22–24) and now unambiguously demonstrated, *Ms*PimA is the first enzyme engaged in the pathway. It is responsible for transferring a Man*p* residue from GDP-Man onto the 2-position of the *myo*-Ins ring of PI to form PIM_1. *Ms*PimB′ then transfers a second Man*p* residue from the same sugar donor to the 6-position of the *myo*-Ins ring of PIM_1 yielding PIM_2. Finally, the acyltransferase MSMEG_2934 acylates the Man*p* residue transferred by PimA to yield one of the major forms of PIM species found in mycobacteria, Ac_1PIM_2.

MsPimB′ Is Essential for the Growth of M. smegmatis—To investigate the essentiality or, on the contrary, possible redundancy of the ManT PimB′ in mycobacteria, a *MspimB′* (*MSMEG_4253*) conditional mutant of *M. smegmatis* mc^2155 was constructed. The methodology employed relies upon a suicide plasmid harboring the counter-selectable marker *sacB* to achieve allelic replacement, and a replicative temperature-sensitive plasmid (pCG76) to express a rescue copy of the gene of interest. Briefly, clones having undergone single crossover at the *MspimB′* locus were first selected upon plating of mc^2155/pJQ*MspimB′KX* transformants on LB-Kan plates at 37 °C. Single crossover recombinants were grown in LB-Kan broth and then plated onto sucrose containing plates at 30 or 37 °C to select for allelic exchange mutants. No knock-out mutants were isolated at this stage strongly suggesting that *MspimB′* was essential for growth regardless of the temperature used. To confirm this assumption, a conditional mutant of *M. smegmatis* was constructed. A temperature-sensitive rescue plasmid carrying a wild type copy of the *MspimB′* gene, pCG*MspimB′*, was introduced in one of the single crossover recombinants, and the resulting merodiploids were plated onto LB-Kan-sucrose plates at 30 °C. Candidate conditional mutants were obtained in which allelic replacement at the chromosomal *MspimB′* locus was confirmed by PCR (Fig. 6*A*). The conditional mutants grew normally at 30 °C in liquid broth or on plates, a temperature at which pCG*MspimB′* replicates, but lost viability at 42 °C where the rescue plasmid is lost (Fig. 6*B*). Results thus indicated that *MspimB′* is essential for the growth of *M. smegmatis* under the

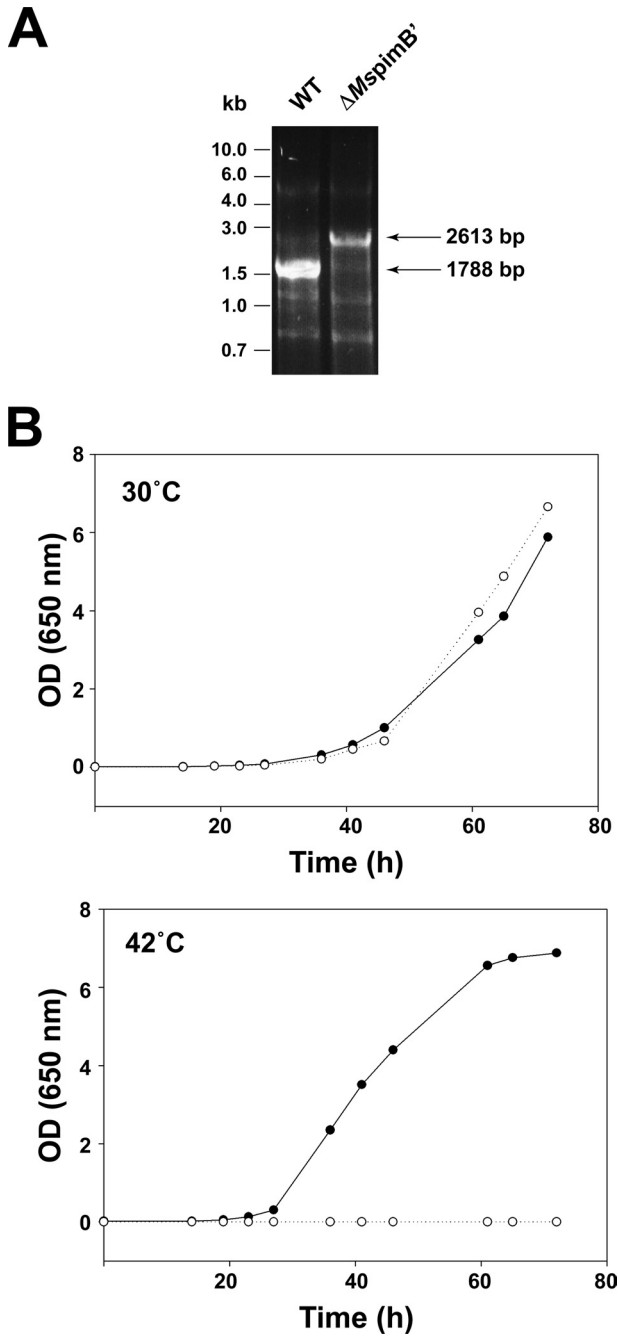

FIGURE 6. **Essentiality of *MspimB′* in *M. smegmatis*.** *A,* PCR analysis showing allelic replacement at the *MspimB′* locus. The wild type (*WT*) 1788-bp fragment is replaced by a 2613-bp fragment in the mutant because of the insertion of a 1.2-kb kanamycin resistance cassette. *B,* growth characteristics of the *MspimB′* conditional mutant (○) and wild-type mc^2155 parent strain (●) at 30 and 42 °C.

experimental conditions used. Therefore, despite the interchangeability of the *M. tuberculosis* PimB and PimB′ enzymes expressed in *C. glutamicum* in cell-free assays (12), the function of *Ms*PimB′ cannot be compensated by any other ManTs, including *Ms*PimB (MSMEG_1113; 75% identical to PimB from *M. tuberculosis* on a 375-residue overlap) in whole *M. smegmatis* cells.

Structural Comparison of MsPimA and MsPimB′—The α-ManTs *Ms*PimA and *Ms*PimB′ belong to the large GT4 fam-

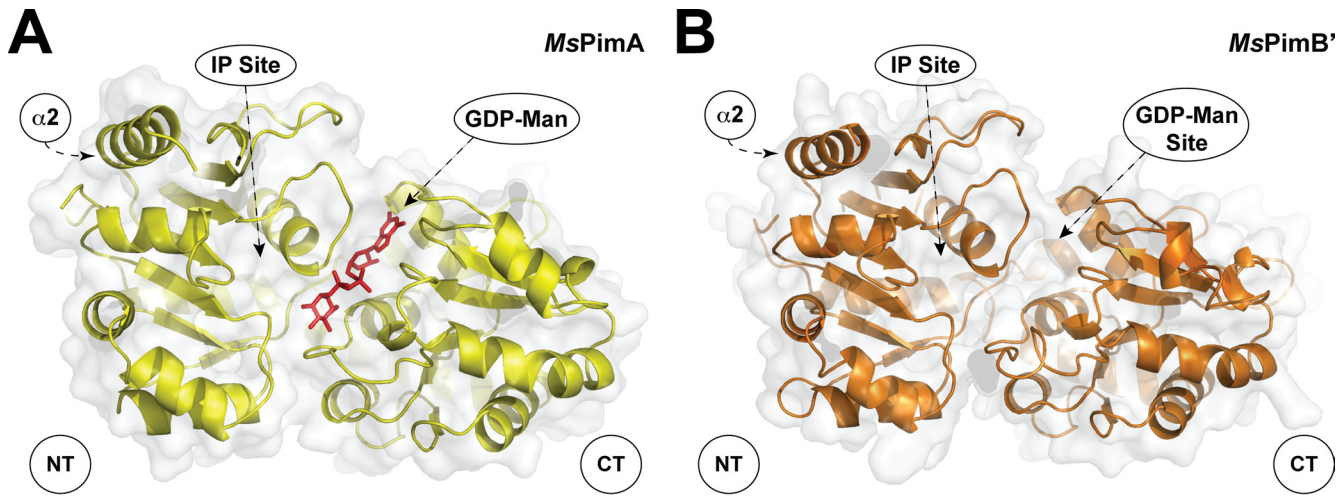
A
MsPimA
IP Site
α2
GDP-Man
NT
CT
B
MsPimB'
IP Site
α2
GDP-Man Site
NT
CT

C

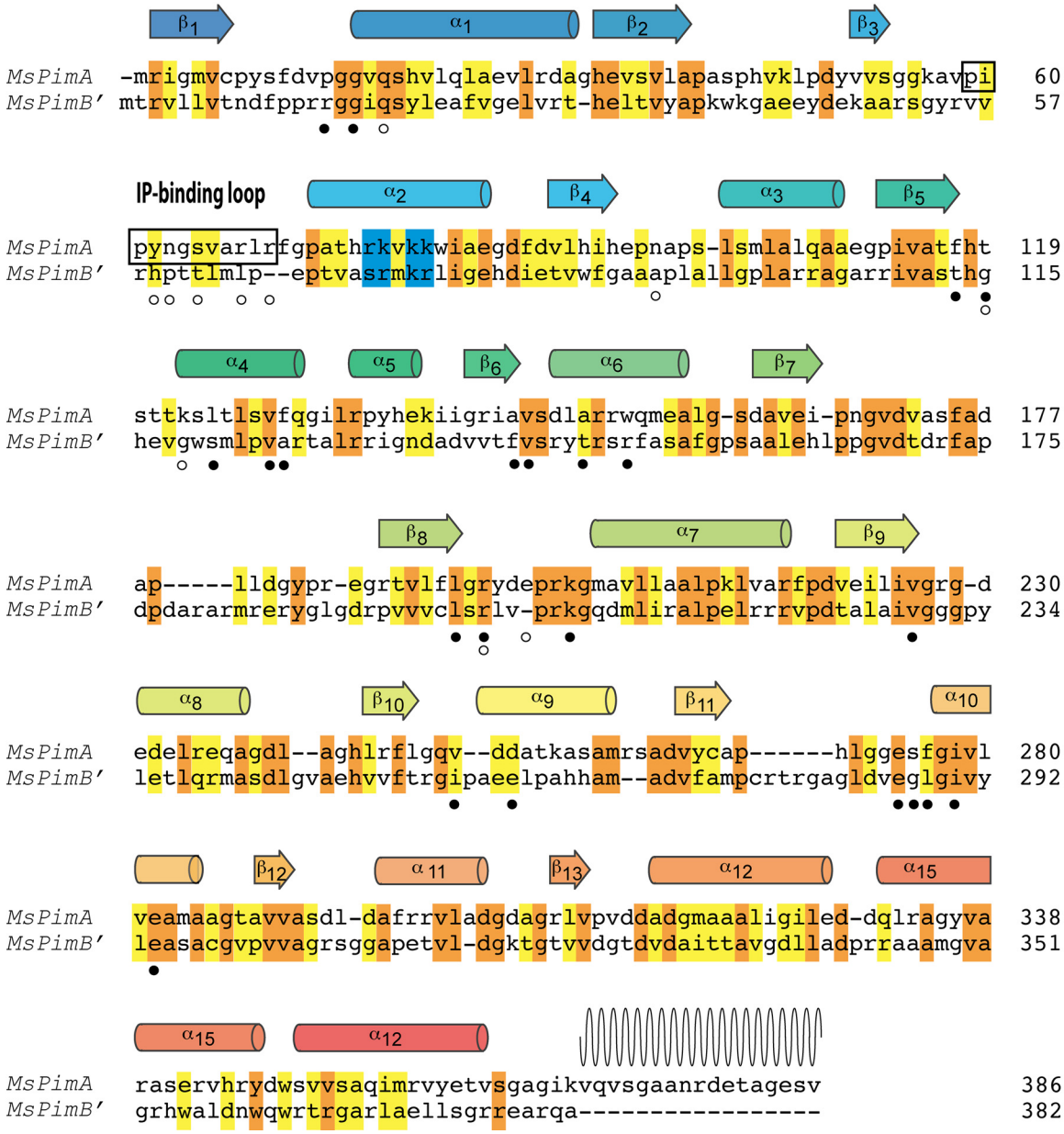
β1 α1 β2 β3
MsPimA -mrigmvcpysfdvpggvqshvlqlaevlrdaghevsvlapasphvklpdyvvsggkavpi 60
MsPimB' mtrvllvtndfpprrggiqsyleafvgelvrt-heltvyapkwkgaeeydekaarsgyrvv 57
IP-binding loop
α2 β4 α3 β5
MsPimA pyngsvarlrfgpathrkvkkwiaegdfdvlhihepnaps-lsmlalqaaegpivatfht 119
MsPimB' rhpttlmlp--eptvasrmkrligehdietvwfgaaaplallgplarragarrivasthg 115
α4 α5 β6 α6 β7
MsPimA sttksltlsvfqgilrpyhekiigriavsdlarrwqmealg-sdavei-pngvdvasfad 177
MsPimB' hevgwsmlpvartalrrignd advvtfvsrytrsrfasafgpsaalehlppgvdtdrfap 175
β8 α7 β9
MsPimA ap-----lldgypr-egrtvlflgrydeprkgmavllaalpklvarfpdveilivgrg-d 230
MsPimB' dpdararmreryglgdrpvvvclsrlv-prkgqdmliralpelrrrvpdtalaivgggpy 234
α8 β10 α9 β11 α10
MsPimA edelreqagdl--aghlrflgqv--ddatkasamrsadvycap------hlggesfgivl 280
MsPimB' letlqrmasdlgvaehvvftrgipaeelpahham--advfampcrtrgagldveglgivy 292
β12 α11 β13 α12 α15
MsPimA veamaagtavvasdl-dafrrvladgdagrlvpvddadgmaaaligiled-dqlragyva 338
MsPimB' leasacgvpvvagrsggapetvl-dgktgtvvdgtdvdaittavgdlladprraaamgva 351
α15 α12
MsPimA raservhrydwsvvsaqimrvyetvsgagikvqvsgaanrdetagesv 386
MsPimB' grhwaldnwqwrtrgarlaellsgrrearqa---------- 382

ily of glycosyltransferases, which includes more than 9800 proteins and at least 12 different enzymatic activities (see the Carbohydrate-Active enZymes data base). The GT4 family contains several enzymes of potential therapeutic significance and has been proposed as the ancestral "retaining" family from which enzymes with this type of stereochemistry have evolved (25, 26). *Ms*PimA is one of the few GT4 enzymes whose three-dimensional structure has been solved. The enzyme displays the GT-B fold that consists of two Rossmann-like β-α-β domains separated by a large cleft that includes the catalytic center (Fig. 7*A*). The GDP-Man-binding site is located mainly in the C-terminal domain, where it makes a number of hydrogen bonds with the protein. Docking calculations and site-directed mutagenesis recently provided clear insights into the position of the polar head of the acceptor substrate, PI. Structural and enzymatic evidence support a model of interfacial catalysis in which *Ms*PimA recognizes PI with its polar head within the catalytic cleft and the fatty acid moieties only partially sequestered from the bulk solvent. Membrane association is mediated by an interfacial binding surface in the N-terminal domain of the protein, which likely includes a cluster of basic residues in the amphipathic α-helix 2 (17) (Fig. 7*A*).

A three-dimensional model of *Ms*PimB′ was generated by homology modeling using the crystal structure of the *Ms*PimA-GDP-Man complex as a template. Given that the two enzymes share only 28% overall sequence identity, the alignment was manually corrected incorporating information such as secondary structure prediction and conservation of functional residues. The overall predicted structure of *Ms*PimB′ strongly resembles the experimental model of *Ms*PimA (Fig. 7, *A* and *B*). Critical residues and their interactions are preserved in the two enzymes strongly supporting conserved catalytic and membrane association mechanisms (Fig. 7*C*). Two hydrophobic residues, Leu^{194} and Val^{226}, that participate in the stabilization of the guanidyl heterocycle of GDP-Man in *Ms*PimA are strictly conserved in *Ms*PimB′ (Leu^{198} and Val^{229}). Similarly, Val^{251} and Asp^{253}, which confer nucleotide specificity to guanosine in *Ms*PimA, are equivalent to Ile^{257} and Glu^{261}, respectively, in *Ms*PimB′. Gly^{16}, Arg^{196}, and Lys^{202}, which are essential to stack the β-PO_4 of GDP-Man in *Ms*PimA, correspond to *Ms*PimB′ residues Gly^{17}, Arg^{200}, and Lys^{205}. Furthermore, Glu^{274} and His^{118}, which are important for catalysis in *Ms*PimA and several other GT-B enzymes, are equivalent to Glu^{286} and His^{114} in *Ms*PimB′ (17). Interestingly, the *Ms*PimB′ model predicts an amphipathic α-helix of the same length (14 residues) as the amphipathic α2 of *Ms*PimA in which Arg^{78}, Lys^{80}, and Arg^{81} are also conserved. However, some of the key residues involved in PI binding, most notably the connecting loop between β3 and α2, differ between the two proteins reflecting their different acceptor substrate specificity. Overall, the structural conservation of *Ms*PimA and *Ms*PimB′ suggests that the two enzymes follow similar molecular mechanisms of substrate/membrane recognition and catalysis.

Concluding Remarks—Altogether, the results of our cell-free assays support a revised model for the early steps of PIM biosynthesis wherein the major PIM product of mycobacteria, Ac_1PIM_2, is formed via the sequential activity of PimA followed by PimB′ and, finally, the acyltransferase MSMEG_2934 (Fig. 5). Evidence is also provided for the first time that PimB′ is the ManT responsible for the addition of the Man*p* residue linked to position 6 of the *myo*-Ins moiety of PI in mycobacteria, and that a deficiency in its activity cannot be compensated by any other ManT of *M. smegmatis*. Thus, despite PimB and PimB′ having the potential to mannosylate the same substrates in *in vitro* assays (12), PimB and PimB′ clearly do not have redundant physiological functions in whole mycobacterial cells.

After PgsA1 (MSMEG_2933, Rv2612c in *M. tuberculosis* H37Rv), PimA (MSMEG_2935, Rv2610c in *M. tuberculosis* H37Rv), and the acyltransferase MSMEG_2934 (Rv2611c in *M. tuberculosis* H37Rv), PimB′ (Rv2188c in *M. tuberculosis* H37Rv) is now the fourth enzyme of the PIM pathway found to be essential in *M. smegmatis* and/or *M. tuberculosis* (5, 13, 27).[5] Although this finding implies that PI, PIM_1, and PIM_2 are essential phospho(glyco)lipids, it is at present difficult to distinguish which of their roles as metabolic end products or as precursors for more mannosylated molecules (LM, LAM, and biosynthetic intermediates) specifically accounts for their essentiality. Ac_1PIM_2 appears to be a metabolic end product that accumulates at high steady state levels in the cells as well as a precursor for more polar forms of PIMs, LM and LAM. Both the PIM_2 and the polar PIM contents of mycobacteria were found to directly impact on the permeability of the cell envelope (4, 5).[6] Moreover, polar PIMs have been implicated in the homeostasis of the plasma membrane (6). In contrast to apolar PIMs, the essentiality of LM, LAM, and biosynthetic intermediates to the physiology of mycobacteria appears to depend on the *Mycobacterium* species. For instance, whereas the arabinosylation of LM was found to be essential to the growth of *M. tuberculosis* (28), this process is not essential to the viability of *M. smegmatis* (29). An *M. smegmatis* knock-out mutant defective in some aspects of the elongation of the mannan backbone of LM was also found to be viable, although its colonial morphology and growth rates were altered (30). Clearly, PIMs, LM, and LAM are likely to be involved in more than one critical function in mycobacterial cells, each of which or the combination of which might account for their essentiality. From a drug development perspective, the essential character of PIM biosynthetic enzymes and their relative restriction to mycobacteria and a few other actinomycetes

[5] G. Stadthagen and M. Jackson, unpublished results.
[6] N. Barilone and M. Jackson, unpublished results.

FIGURE 7. **Structural similarity between *Ms*PimA and *Ms*PimB′.** *A,* experimental three-dimensional model of the crystal structure of *Ms*PimA. *B,* three-dimensional homology model of *Ms*PimA (Protein Data Bank code 2GEJ, see Ref. 17). *C,* structural alignment of *Ms*PimA and *Ms*PimB′. Secondary structure elements of the *Ms*PimA three-dimensional structure are shown *above* the protein sequence. *Wavy lines* indicate disordered regions in the three-dimensional structure. The basic cluster in helix α2, which is proposed to be involved in membrane interaction, is highlighted in *blue*. Identical residues are shown in an *orange background*, and homologous residues are shown in a *yellow background*. Residues involved in the binding of GDP-Man and PI are denoted with *solid* and *open circles*, respectively.

emphasizes their interest as novel targets for anti-tuberculosis chemotherapeutic agents.

Acknowledgments—We gratefully acknowledge Dr. Karolin Luger (Department of Biochemistry and Molecular Biology, Colorado State University) for access to the protein purification facility, Dr. Hataichanok Scherman for help with plasmid constructs, and Dr. Jiang Zhang (Department of Microbiology, Immunology, and Pathology, Colorado State University) for help with NMR experiments.

REFERENCES

1. Gilleron, M., Jackson, M., Nigou, J., and Puzo, G. (2008) in *The Mycobacterial Cell Envelope* (Daffé, M., and Reyrat, J. M., eds) pp. 75–105, American Society for Microbiology, Washington, D. C.
2. Kaur, D., Guerin, M. E., Skovierova, H., and Jackson, M. (2009) *Adv. Appl. Microbiol.,* in press
3. Goren, M. B. (1984) in *The Mycobacteria: A Sourcebook* (Kubica, G. P., and Wayne, L. G., eds) Vol. 1, pp. 379–415, Marcel Dekker, Inc., New York
4. Parish, T., Liu, J., Nikaido, H., and Stoker, N. G. (1997) *J. Bacteriol.* **179,** 7827–7833
5. Korduláková, J., Gilleron, M., Mikusova, K., Puzo, G., Brennan, P. J., Gicquel, B., and Jackson, M. (2002) *J. Biol. Chem.* **277,** 31335–31344
6. Morita, Y. S., Sena, C. B., Waller, R. F., Kurokawa, K., Sernee, M. F., Nakatani, F., Haites, R. E., Billman-Jacobe, H., McConville, M. J., Maeda, Y., and Kinoshita, T. (2006) *J. Biol. Chem.* **281,** 25143–25155
7. Schaeffer, M. L., Khoo, K. H., Besra, G. S., Chatterjee, D., Brennan, P. J., Belisle, J. T., and Inamine, J. M. (1999) *J. Biol. Chem.* **274,** 31625–31631
8. Kremer, L., Gurcha, S. S., Bifani, P., Hitchen, P. G., Baulard, A., Morris, H. R., Dell, A., Brennan, P. J., and Besra, G. S. (2002) *Biochem. J.* **363,** 437–447
9. Torrelles, J. B., Desjardin, L. E., MacNeil, J., Kaufman, T. M., Kutzbach, B., Knaup, R., McCarthy, T. R., Gurcha, S. S., Besra, G. S., Clegg, S., and Schlesinger, L. S. (2009) *Glycobiology* **19,** 743–755
10. Tatituri, R. V., Illarionov, P. A., Dover, L. G., Nigou, J., Gilleron, M., Hitchen, P., Krumbach, K., Morris, H. R., Spencer, N., Dell, A., Eggeling, L., and Besra, G. S. (2007) *J. Biol. Chem.* **282,** 4561–4572
11. Lea-Smith, D. J., Martin, K. L., Pyke, J. S., Tull, D., McConville, M. J., Coppel, R. L., and Crellin, P. K. (2008) *J. Biol. Chem.* **283,** 6773–6782
12. Mishra, A. K., Batt, S., Krumbach, K., Eggeling, L., and Besra, G. S. (2009). *J. Bacteriol.* **191,** 4465–4472
13. Korduláková, J., Gilleron, M., Puzo, G., Brennan, P. J., Gicquel, B., Mikusová, K., and Jackson, M. (2003) *J. Biol. Chem.* **278,** 36285–36295
14. Guerin, M. E., Buschiazzo, A., Korduláková, J., Jackson, M., and Alzari, P. M. (2005) *Acta Crystallogr. Sect. F Struct. Biol. Cryst. Commun.* **61,** 518–520
15. Guilhot, C., Otal, I., Van Rompaey, I., Martìn, C., and Gicquel, B. (1994) *J. Bacteriol.* **176,** 535–539
16. Martí-Renom, M. A., Stuart, A. C., Fiser, A., Sánchez, R., Melo, F., and Sali, A. (2000) *Annu. Rev. Biophys. Biomol. Struct.* **29,** 291–325
17. Guerin, M. E., Kordulakova, J., Schaeffer, F., Svetlikova, Z., Buschiazzo, A., Giganti, D., Gicquel, B., Mikusova, K., Jackson, M., and Alzari, P. M. (2007) *J. Biol. Chem.* **282,** 20705–20714
18. Cuff, J. A., and Barton, G. J. (2000) *Proteins Struct. Funct. Genet.* **40,** 502–511
19. Gilleron, M., Nigou, J., Cahuzac, B., and Puzo, G. (1999) *J. Mol. Biol.* **285,** 2147–2160
20. Gilleron, M., Ronet, C., Mempel, M., Monsarrat, B., Gachelin, G., and Puzo, G. (2001) *J. Biol. Chem.* **276,** 34896–34904
21. Gilleron, M., Quesniaux, V. F., and Puzo, G. (2003) *J. Biol. Chem.* **278,** 29880–29889
22. Hill, D. L., and Ballou, C. E. (1966) *J. Biol. Chem.* **241,** 895–902
23. Brennan, P., and Ballou, C. E. (1967) *J. Biol. Chem.* **242,** 3046–3056
24. Takayama, K., and Goldman, D. S. (1969) *Biochim. Biophys. Acta* **176,** 196–198
25. Martinez-Fleites, C., Proctor, M., Roberts, S., Bolam, D. N., Gilbert, H. J., and Davies, G. J. (2006) *Chem. Biol.* **13,** 1143–1152
26. Lairson, L. L., Henrissat, B., Davies, G. J., and Withers, S. G. (2008) *Annu. Rev. Biochem.* **77,** 521–555
27. Jackson, M., Crick, D. C., and Brennan, P. J. (2000) *J. Biol. Chem.* **275,** 30092–30099
28. Goude, R., Amin, A. G., Chatterjee, D., and Parish, T. (2008) *J. Bacteriol.* **190,** 4335–4341
29. Zhang, N., Torrelles, J. B., McNeil, M. R., Escuyer, V. E., Khoo, K. H., Brennan, P. J., and Chatterjee, D. (2003) *Mol. Microbiol.* **50,** 69–76
30. Kaur, D., McNeil, M. R., Khoo, K. H., Chatterjee, D., Crick, D. C., Jackson, M., and Brennan, P. J. (2007) *J. Biol. Chem.* **282,** 27133–27140